Bioconjugate Chemistry

Article

pubs.acs.org/bc

Creation of Artificial Luciferases for Bioassays

Sung Bae Kim,* Masaki Torimura, and Hiroaki Tao

[1]Research Institute for Environmental Management Technology, National Institute of Advanced Industrial Science and Technology (AIST), 16-1 Onogawa, Tsukuba 305-8569, Japan

Supporting Information

ABSTRACT: The present study demonstrates the creation of artificial luciferases (ALuc) for bioassays, inspired by a sequence alignment of copepod luciferases. Extraction of the consensus amino acids from the alignment enabled us to generate a series of ALucs with unique optical properties and sequential identities that are clearly different from those of any existing copepod luciferase. For example, some ALucs exhibited heat stability, dramatically prolonged optical intensities, broad full width at half-maximum, and strong optical intensities. The practical suitability of the luciferases as an optical readout was examined in diverse bioassays, including mammalian two-hybrid assays, live cell imaging, single-chain probes, bioluminescent capsules, and bioluminescent antibodies. We further determine the physical properties of ALucs through bioinformatic analysis and finally discuss detailed issues on the unique properties of ALucs. The present study shows how to create the artificial enzymes with excellent optical properties for bioassays and encourages researchers to fabricate their own unique artificial enzymes with designed properties and functionalities.

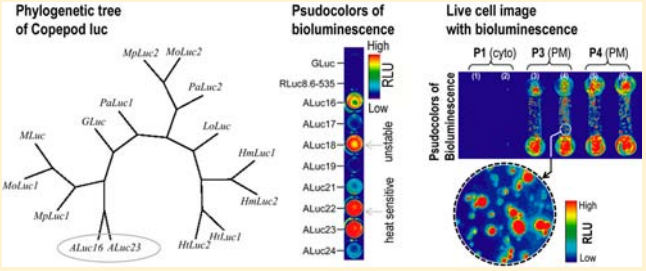

INTRODUCTION

Luciferases are a family of light-generating proteins that can be isolated from a large variety of insects, marine organisms, and prokaryotes.[1,2] The light-emitting mechanisms are also intensively investigated through analysis of the crystallographic data[3] and organic synthesis of the substrates.[4]

Although our knowledge on luciferases is rapidly emerging, the practical strategy to engineer luciferases has been confined to mutagenesis. Either point or random mutagenetic approaches are generally slow and tedious, and they consume much time and labor. Crystallographic information on luciferases is also rarely available.[5] Exceptionally, a fluorescent protein-linked luciferase successfully generated artificial bioluminescence via a bioluminescence resonance energy transfer (BRET).[6]

Alternatively, an alignment of many relative protein sequences in public databases facilitates new insights on the phylogenetic history, structural information, consensus amino acids, as well as functional motifs. One of the major strategies using a sequence alignment is the "*consensus sequence-driven mutagenesis strategy*" (CSMS), in which homologous protein sequences are aligned to find consensus amino acids and mutagenesis sites.[7,8] This approach is based on the premise that frequently occurring amino acids at a given position have a larger thermostabilizing effect than less frequent amino acids do. A more precise bioinformatics analysis of multiple sequence alignments, called "*statistical coupling analysis* (SCA)", was also developed to explain the evolutionary constraints of proteins by measuring the relative entropy (D_i) of an amino acid.[9] We had also suggested that a putative core region of marine luciferases may be highlighted by a hydrophobicity search and an overlapping approach of the two domains of copepod luciferases, called "*single-sequence alignment* (SSA)".[5]

When we review the precedent knowledge on luciferase engineering, our fundamental curiosity concerns the question of why we do not construct whole sequences of artificial luciferases (ALuc) that have never existed, instead of undertaking heavily labor-consuming mutagenesis of existing luciferases. This view prompted us to create a series of ALucs with a strategy of whole-scale construction of consensus amino acid sequences from an alignment of many existing luciferases in a public database, i.e., the National Center for Biotechnology Information (NCBI), whose sequences have been accumulated by great devotion of many researchers. The validity of this idea was examined with an alignment of 13 copepod luciferases in the public domain,[10] from which frequently occurring amino acids were extracted to reconstitute a prototypical sequence of ALucs. Copepod luciferases are an ideal model for the present purpose, because (i) the luciferase sequences are highly conserved, (ii) they exhibit the smallest molecular weights among existing luciferases, and (iii) they are supposed to consist of two repeated catalytic domains,[11] with the alignment of the two catalytic domains additionally revealing consensus amino acids. This SSA alignment helps in deciding appropriate amino acids in the variable regions.

Using the above-mentioned process, we created a series of ALucs, the maximal sequence identities of which were below 83% according to the NCBI Blast and less than 76% according

Received: September 2, 2013
Revised: November 10, 2013
Published: November 18, 2013

dx.doi.org/10.1021/bc400411h | *Bioconjugate Chem.* 2013, 24, 2067−2075

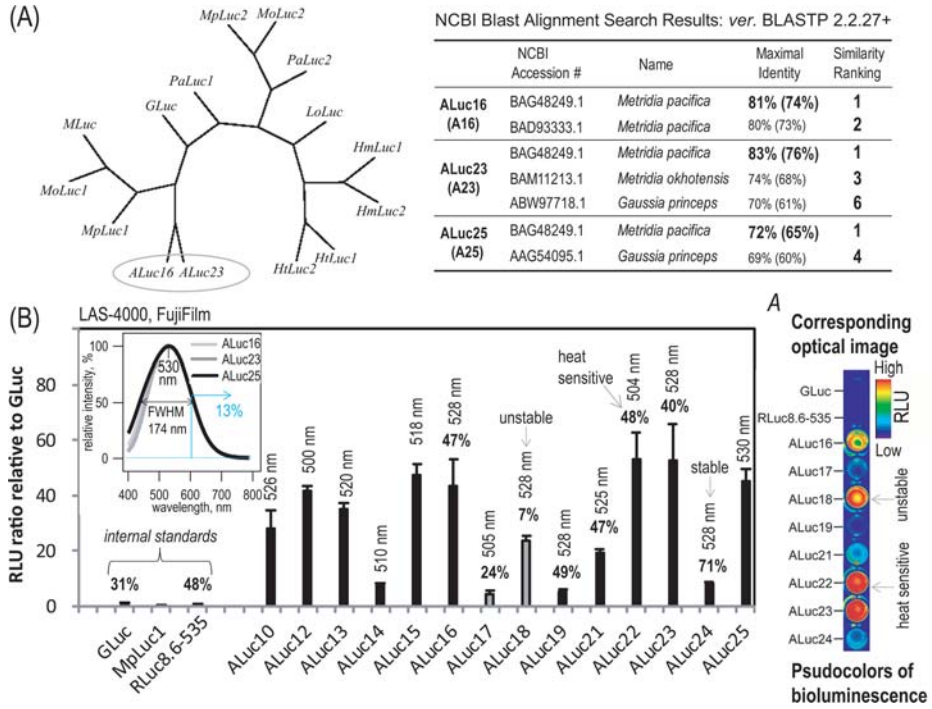

Figure 1. Creation of artificial luciferases. (A) An unrooted phylogenetic tree according to CLUSTALW v 2.1 (left). The circle indicates the relative positions of **A16** and **A23** in the tree. The sequences of copepod luciferases were obtained from a public database, NCBI Blast. Identical sequences to ALucs were also searched with public alignment services (NCBI Blast and SIB Blast) (right table). The percentages in the parentheses demonstrate the corresponding results from SIB Blast as another database service. (B) Relative optical intensities of ALucs, compared with GLuc (n = 3). The gray bars indicate relatively unstable ALucs. The inset shows the representative bioluminescence spectra obtained with a high precision spectrophotometer (AB1850; ATTO). FWHM means full width at half-maximum. Section *A* shows the pseudocolor image of the bioluminescence generated by ALucs, obtained using an image analyzer (LAS-4000, FujiFilm).

to the Swiss Institute of bioinformatics (SIB) Blast, compared with any existing luciferases in the public databases. The optical intensities were ca. 50 times stronger than any existing copepod luciferases and were extremely stable and with red-shifted bioluminescence. We further examined the suitability of these luciferases as an optical readout in bioassays and determined the physical properties through a bioinformatics analysis.

EXPERIMENTAL SECTION

Construction of Artificial Luciferases. The murine codon-optimized cDNA sequences encoding ALucs were custom-synthesized according to the alignment of Figures S1 and S2, where the sequences were determined through the following procedure: (i) The consensus amino acids were first determined from the alignment of known copepod luciferase sequences to make a prototype of a series of ALucs (Figure S1). The majority of amino acids in the conserved regions were adjusted in the light of the precedent view that copepod luciferases have two repeated catalytic domains, i.e., SSA. The alignment reveals two repeated catalytic domains. Considering that the two repeated domains are mirror images of each other, some amino acids in a catalytic domain were adjusted in light of the corresponding amino acids in the other domain (arrows in Figure S1). The remaining amino acids in the variable region were decided on an occasional basis to complete the prototype. The prototypical sequence was then utilized to generate a series of the potential sequences of ALucs (Figure S2). (ii) The codons encoding the sequences were murinized for their optimal expression in murine cells. (iii) Because copepod luciferases are supposed to have a secretion peptide at the N-terminal end, an endoplasmic reticulum (ER) retention signal, i.e., KDEL, was added at the C-terminal end of the made sequence for the retention in the ER. The average length and molecular weight (MW) of the made sequences were 207 (±10 s.d.) AAs and 22.4 (±1.0 s.d.) kD, respectively.

The cDNAs encoding each ALuc were custom-synthesized on order by Operon Biotechnology (Tokyo, Japan). The synthesized cDNAs were subcloned into pcDNA3.1(+) (Invitrogen) using the specific restriction sites, *Hind*III and *Xho*I, for expression in mammalian cells. The overall sequence fidelity was confirmed with a sequencing service provided by Operon Biotechnology (Tokyo, Japan).

Maximal identity and similarity ranking of the ALuc sequences in the absence of KDEL, compared with existing luciferases, were determined using an alignment search tool provided by NCBI Blast (v BLASTP 2.2.27+; http://www.ncbi.nlm.nih.gov/) and SIB Blast (http://web.expasy.org/blast). The table of Figure 1(A) lists the results.

Relative Optical Intensities of ALucs Compared with Those of GLuc. The relative optical properties of ALucs were examined in COS-7 cells derived from African green monkey kidney fibroblast, which is grown in Dulbecco's minimal essential medium (DMEM) (Gibco) supplemented with 10% heat-inactivated fetal bovine serum (FBS) (Gibco) and 1% penicillin/streptomycin (P/S) (Gibco) (Figure 1(B)).

COS-7 cells grown in a 96-well plate (Nunc) were transiently transfected with the pcDNA3.1(+) plasmids encoding each ALuc (Figure S2(A)) or existing marine luciferases, i.e., *Gaussia princeps* luciferase (Gluc; GenBank AAG54095.1),[12] *Metridia pacifica* luciferase 1 (MpLuc1; GenBank AB195233),[13] or *Renilla reniformis* luciferase 8.6−535 (RLuc8.6-535)[14] as the internal references using a lipofection reagent, TransIT-LT1

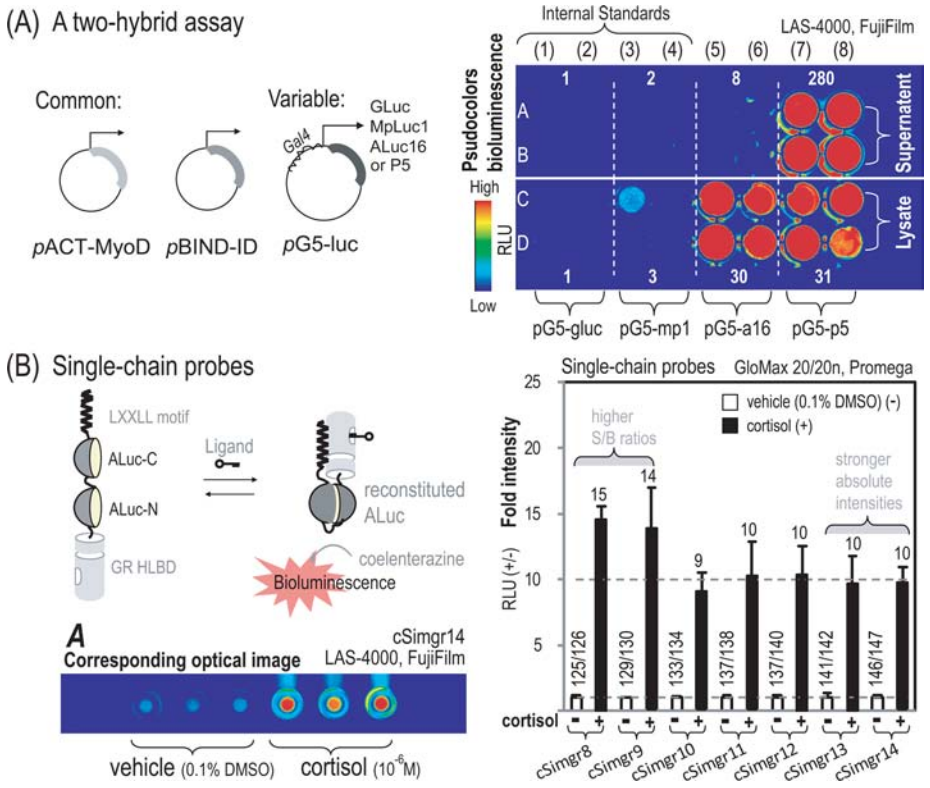

Figure 2. Applications of ALucs to mammalian two-hybrid assays and single-chain probes. (A) Determination of MyoD−ID interactions using a mammalian two-hybrid assay system (Checkmate, Promega) (n = 4). Spontaneous interaction between MyoD and ID provokes the expression of the respective reporters, GLuc, MpLuc1 (mp1), **A16**, and **P5**, from each pG5 vector. The numbers on the optical image show the relative optical intensities of the bioluminescence, compared to GLuc. (B) Determination of stress hormone (cortisol) levels with single-chain probes carrying **A16** fragments split at diverse dissection sites (n = 3). The left column illustrates the working mechanism of the single-chain probes before and after the addition of cortisol. Cortisol restores the optical intensities of the probes through the reconstitution of the fragmented **A16**. The right column indicates the S/B ratio of each single-chain probe carrying a different **A16** fragment dissected at the specified site. The numbers on the black bars show the fold intensities with cortisol, compared with those without cortisol.

(Mirus). Sixteen hours after the transfection, the cells on each well were lysed with 50 μL of a lysis buffer (E291A; Promega). An aliquot of the lysates (10 μL) was transferred into two separated 96-well plates (Nunc) using an 8-channel pipet: one of the plates was used for determining the relative bioluminescence intensities, while the other was for the adjustment of variance of the protein amounts (control). The relative bioluminescence intensities were determined after a programmed, automatic injection of the specific substrate, native coelenterazine (nCTZ; Promega), dissolved in an RLuc assay buffer (E290B, Promega) using a microplate reader equipped with an automatic injector (SH-9000lab, Corona). The luminescence intensities were normalized to that of GLuc as an internal reference to show them in relative fold intensity.

The bioluminescence spectra from the above-prepared lysates were estimated with a high-fidelity spectrophotometer (AB-1850, ATTO) equipped with a cooled charge-coupled device (CCD) camera that enables one-shot capture of the entire light. The lysate (5 μL) was mixed with 50 μL of the RLuc assay buffer carrying nCTZ (E2820, Promega) and immediately placed in the instrument for the measurement. The integration time was 10 s. The spectra were normalized in relative percentages (Figure 1(B), inset).

The optical images from the above prepared lysates were also determined with an image analyzer (LAS-4000, FujiFilm) immediately after a simultaneous injection of 40 μL of the RLuc assay buffer carrying nCTZ to each well carrying 10 μL of the lysates using a multichannel pipet (Figure 1(B), inset A). The optical intensities were normalized in relative intensities compared to GLuc as the internal reference.

Two-Hybrid Assay. The suitability of ALucs as an optical readout was examined with a mammalian two-hybrid assay system (Checkmate, Promega) expressing RLuc8.6-535, MpLuc1, ALuc16 (**A16**), and A16-DEVD-MLS (Figure 2(A)). For the present two-hybrid assay, we first made a new plasmid set by replacing the cDNA encoding firefly luciferase (FLuc) in a commercial plasmid called 'pG5luc' (Promega) with one encoding GLuc, MpLuc1,[15] **A16**, or **P5** (i.e., A16-DEVD-MLS). The plasmids were named pG5-gluc, pG5-mp1, pG5-a16, and pG5-p5, respectively.

COS-7 cells stably expressing MyoD were established with pACT-MyoD (Neo) (Promega) using the culture medium supplemented with G418 (final conc: 0.5 mg/mL). The cells stably expressing MyoD were grown to 90% confluence in wells of a 96-well microplate. The cells were further transiently cotransfected with the following two plasmids: common pBIND-ID (Promega) vector and one of pG5-gluc, pG5-mp1, pG5-a16, or pG5-p5. Twenty hours after the transfection, 20 μL of the supernatants of the cells were separately stocked to determine the relative intensities of the secreted reporters. The remaining cells were washed once with a PBS buffer and lysed with 50 μL of a lysis buffer (E291A, Promega) for 20 min. The lysates (10 μL) were transferred to a new microplate for the activity measurement. The optical intensities of the super-

dx.doi.org/10.1021/bc400411h | Bioconjugate Chem. 2013, 24, 2067−2075

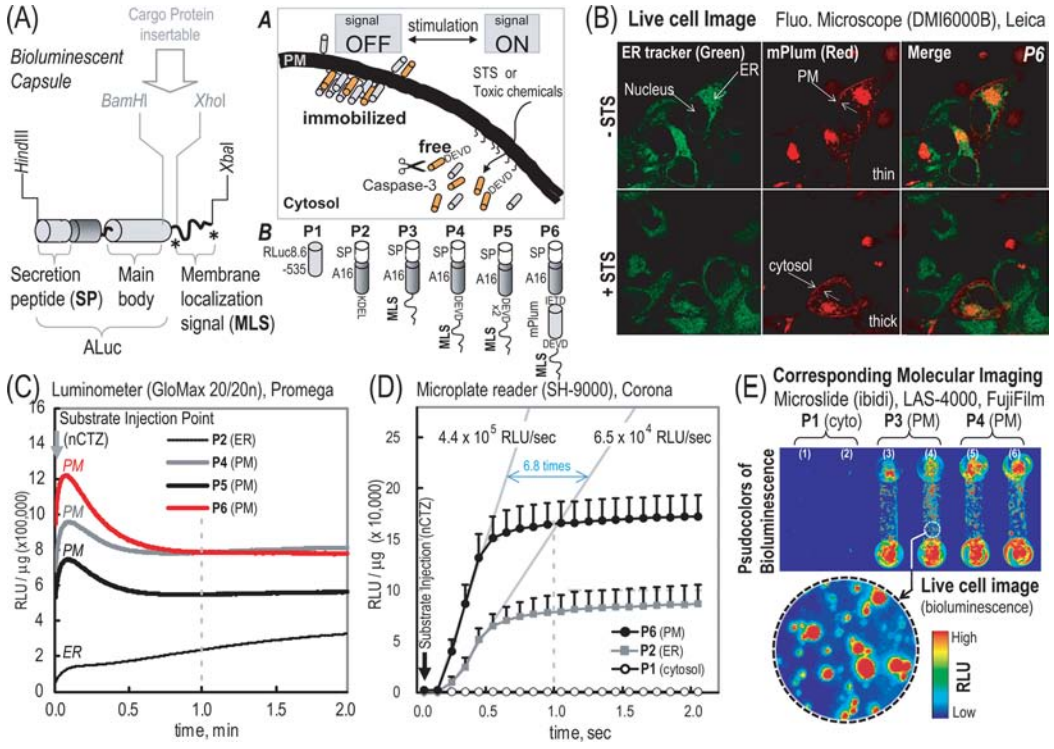

Figure 3. Bioluminescent capsules and their applications to live cell imaging. (A) Cartoon illustration of the molecular structures of the presently constructed capsules. Inset *A* shows the working mechanisms of a capsule, **P6**, anchoring in the PM. A capsule is diffused to the cytosol by an apoptosis signal. Inset *B* illustrates the molecular structures of various bioluminescent capsules bearing different cargo proteins. (B) Molecular imaging of living mammalian cells with fluorescence. The red fluorescence indicates locating of **P6** in living COS-7 cells before and after stimulation of STS. **P6** is located in the PM or the ER in the basal condition. **P6** releases **A16** to the cytosol in the presence of STS. The blue fluorescence shows the regions of the ER and the Golgi apparatus. The corresponding movies are also available on the Supporting Information. (C) A minute-scale time course of the optical intensities of **P2**, **P4**, **P5**, and **P6** after automatic injection of the specific substrate, *n*CTZ, dissolved in an assay buffer (Promega) (n = 3). The optical intensity of ER-localizing **P2** was generally poor compared with the others. (D) A second-scale time course of the optical intensities of **P1**, **P2**, and **P6** after automatic injection of the specific substrate *n*CTZ (n = 3). The speeds varied dramatically between the PM-localized **P6** and the ER-anchoring **P2**, although they commonly bear **A16**. (E) Molecular imaging of living mammalian cells with bioluminescence. The optical image of a six-channel microslide growing COS-7 cells, which transiently express **P1**, **P3**, or **P4**. The cell territories were visualized with bioluminescence. Abbreviations: STS, staurosporine; SP, secretion peptide; nCTZ, native coelenterazine; RLU, relative luminescence unit; ER, endoplasmic reticulum; PM, plasma membrane.

natants and the lysates relative to GLuc and MpLuc1 (internal standard) were determined with an image analyzer (LAS-4000, FujiFilm) after simultaneous injection of nCTZ using a multichannel pipet (Eppendorf). The integration times for the supernatant and lysates were 16 and 4 min, respectively.

Single-Chain Probes. For the experiment of Figure 2(B), we created a series of cDNA constructs encoding single-chain probes carrying a pair of **A16** fragments split at consecutive dissections sites, as specified in Figure S2(A), and subcloned into pcDNA3.1(+) (Invitrogen). The specific experimental procedure of the generation of the constructs was described in the Supporting Information section. The plasmids were named pcSimgr8 to pcSimgr14 according to the consecutive dissection sites of **A16**.

Stress hormone (cortisol) sensitivity was examined through the following procedure: COS-7 cells grown in the wells of a 96-well plate were transiently transfected with an aliquot of one of the plasmids from pcSimgr8 to pcSimgr14 (0.1 μg per well) using a lipofection reagent (TransIT-LT1, Mirus). Sixteen hours after the transfection, the cells were stimulated for 20 min with vehicle (culture media comprising 0.1% DMSO) or 10^{-6} M of cortisol. The relative optical intensities were determined with a luminometer (GloMax 20/20n, Promega) after lysis of the cells with a lysis buffer (E291A, Promega) and the subsequent injection of the assay buffer carrying the specific substrate, nCTZ, provided by a luciferase assay kit (E2820, Promega). The mixing ratio was 20 μL:50 μL of lysate:assay buffer, and the integration time was 2 s.

In the above study and others, the luminescence intensities were normalized by two methods: (i) one was by the amount of proteins in cell lysates. The unit of absolute luminescence is subsequently RLU/ μg of protein. (ii) The other was expressed by a relative luminescence unit (RLU) ratio ($\pm$), where RLU (+) and RLU (-) represent the luminescence intensity from a 1 μg protein of cell lysate after COS-7 cells were stimulated with and without a ligand, respectively.

A corresponding optical image before and after a cortisol stimulation was also determined using a 6-channel microslide (2.5 × 7.5 cm^2, μ-slide VI$^{0.4}$, ibidi) and an image analyzer (LAS-4000, FujiFilm) (Figure 2(B), inset *A*). The specific experimental procedure was described in the Supporting Information section.

Bioluminescent Capsules. The suitability of ALucs for bioassays was evaluated with bioluminescent capsules, which were designed to carry a membrane localization signal (MLS) for anchoring in the plasma membrane (PM) of mammalian cells (Figure 3). The basic concept was described in our previous study.[16]

dx.doi.org/10.1021/bc400411h | *Bioconjugate Chem.* 2013, 24, 2067−2075

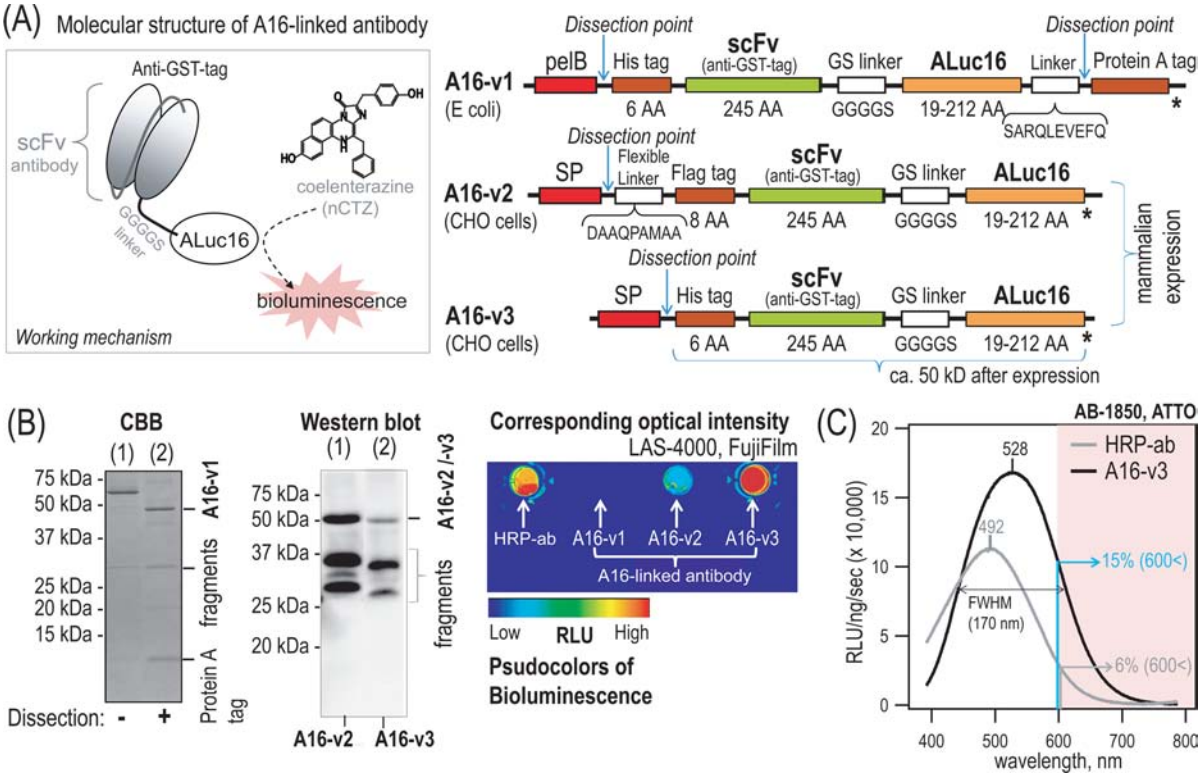

Figure 4. Construction of bioluminescent antibodies and their optical properties. (A) The molecular structures of antibodies, named **A16-v1**, **A16-v2**, and **A16-v3**. The left column demonstrates the lighting mechanism of the **A16**-linked antibodies. The C-terminal end of an anti-GST-tag antibody was fused to **A16**, which lumineses in the presence of nCTZ. The right column shows cDNA constructs of the antibodies. scFv means single-chain variable fragments. (B) The optical images of (i) Coomassie brilliant blue (CBB) staining of **A16-v1** (left column), (ii) Western blotting of **A16-v2** and **A16-v3** (middle column), and (iii) bioluminescence imaging of **A16-v1**, **A16-v2**, and **A16-v3** (right column). The CBB staining shows all the proteins purified, before and after the dissection of the affinity tag, Protein A. The left and right lanes in the Western blot image show the protein bands recognized by anti-FLAG-Tag (MBL) and anti-His-tag antibodies, respectively. The bioluminescence image at the right column indicates the relative optical intensities of 1 μg/mL of HRP or antibodies in pseudocolor. (C) The normalized bioluminescence spectra generated by **HRP-ab** and **A16-v3**. **A16-ab** exerted a stronger red-shifted optical intensity than **HRP-ab** (n = 2).

For the present study, we newly synthesized a series of bioluminescent capsules (Figure 3(A), inset *B*). The generated plasmids were named pP1 to pP6 according to the structure, as shown in Figure 3(A). The specific experimental procedure of the generation of the constructs was described in the Supporting Information section.

A signal-dependent release of the cargo, mPlum, from the capsules in living COS-7 cells was determined with a fluorescent microscope (DMI6000B, Leica) (Figure 3(B)). The 3D movies are available in the Supporting Information.

For the experiment, COS-7 cells were grown in a 3.5 cm glass-bottom dish (Iwaki) and were transiently transfected with pP6. Twenty-four hours after the transfection, the ER regions of the cells were stained green with an ER tracker (Invitrogen) according to the manufacturer's instruction. The cells expressing **P6** were then stimulated with a vehicle (PBS buffer) or 5 μM of staurosporine (STS) for 20 min. The culture media were replaced with a Hank's balanced salt solution (HBSS, Gibco) buffer. The localization regions of the ER and the capsules were imaged with a fluorescent microscope equipped with a 510−530 nm band-pass filter (green, the ER) and 600 nm long-pass filter (red, mPlum) (Figure 3(B)).

The optical stability of **P2**, **P4**, **P5**, and **P6** in living COS-7 cells was also examined using a conventional luminometer (GloMax 20/20n, Promega) (Figure 3(C)). COS-7 cells grown in 3.5 cm glass-bottom dishes (Iwaki) were transiently transfected with an aliquot (0.2 μg) of pP2 (locating in the ER), pP4 (locating in the PM), pP5 (locating in the PM), or pP6 (locating in the PM), and incubated for 16 h. The culture media in the dishes were replaced with an HBSS buffer (Gibco) and set in the luminometer. The time course of the optical intensities was recorded after an automatic injection of nCTZ dissolved in an HBSS buffer. The luminescence intensities were normalized by the total amounts of proteins, which were estimated with a Bradford reagent (BIO-RAD). The unit of absolute luminescence is subsequently relative luminescence unit per microgram (RLU/μg) of protein.

The kinetics of the bioluminescence intensities from living COS-7 cells were similarly determined with a microplate reader (SH-9000lab, Corona) (Figure 3(D)). COS-7 cells carrying **P1** (locating in the cytosol), **P2** (locating in the PM), or **P6** (locating in the PM) were grown in a 96-well plate. The COS-7 cells were washed once with the HBSS buffer and dried up by tapping the microplate before the measurement. The optical intensities from the COS-7 cells were monitored with a 0.1 s interval after a programmed automatic injection of the specific substrate nCTZ dissolved in the HBSS buffer. The obtained luminescence intensities were normalized by the total protein amounts of the lysates of the cells using a Bradford reagent (BIO-RAD).

As supplementary data, the relative optical intensities of the capsules in living COS-7 cells were estimated with an image

dx.doi.org/10.1021/bc400411h | *Bioconjugate Chem.* 2013, 24, 2067−2075

analyzer (LAS-4000, FujiFilm) (Figure 3(E)). COS-7 cells were grown in a 6-channel microslide (ibidi) and transiently transfected with pP1, pP3, and pP4. Sixteen hours after the transfection, the cells in the channels were washed once with an HBSS buffer (Gibco) and then filled with 80 μL of an HBSS buffer dissolving nCTZ using a multichannel pipet for an immediate determination of the optical image in the image analyzer (standard exposure mode, 5 min integration).

Bioluminescent Antibodies. The optical properties of ALuc-linked antibodies were compared with those of a horseradish peroxidase (HRP)-linked antibody (Figure 4).

For the present study, we custom-synthesized ALuc-fused divalent single-chain variable fragments (di-scFv) with the help of an antibody manufacturer, MBL (Nagoya, Japan). Figure 4(A) briefly illustrates the molecular structure, working mechanism, and cDNA constructs. We prepared three purification schemes for the antibodies, whose N- and C-terminal ends were linked with distinctive tags, as shown in Figure 4(A). The corresponding antibodies were named **A16-v1**, **A16-v2**, and **A16-v3**. We first examined the feasibility of a large-scale expression of **A16-v1** in *E. coli*. In parallel, we tested a mammalian cell expression of **A16-v2** and **A16-v3** in Chinese hamster ovary (CHO) cells (Figure 4(B)). The antibodies in the culture media were purified with the corresponding affinity columns, i.e., protein A-tag, IgG-Sepharose, and/or Ni-NTA-Agarose columns. The relative amounts and fragmentation of the purified antibodies were then examined with Coomassie brilliant blue (CBB) staining or Western blot analysis. **A16-v1** bands were blotted with a CBB staining reagent (BIO-RAD) after SDS-polyacrylamide gel electrophoresis (SDS-PAGE), whereas **A16-v2** and **A16-v3** bands were transferred to a nitrocellulose paper (Millipore) and blotted with an anti-FLAG-Tag antibody (MBL) and an anti-His-tag antibody (MBL), respectively, after PAGE.

The relative optical intensities of **A16-v1**, **A16-v2**, and **A16-v3** compared to an HRP-linked antibody (named **HRP-ab**; GE Healthcare) were further examined with an image analyzer (FujiFilm) (Figure 4(B)). Before the comparison, the antibody amounts (**A16-v1**, **A16-v2**, **A16-v3**, and **HRP-ab**) were normalized to be equal with an HBSS buffer or a PBS buffer (final conc: 1 μg/mL). An aliquot of the diluted solutions (5 μL) was then transferred to a 96-well plate (Nunc) and simultaneously mixed with 95 μL of the following substrate solutions using a multichannel pipet (Eppendorf): (i) Immunostar LD (Wako) for the **HRP-ab** and (ii) a bioluminescence assay kit (E2820, Promega) for **A16-v1**, **A16-v2**, and **A16-v3**. The developed bioluminescence intensities were determined with LAS-4000 (FujiFilm) in high-resolution mode with 1 s of the integration time.

The corresponding bioluminescence spectra of **A16-v3** and **HRP-ab** were determined with a spectrophotometer (AB-1850, ATTO) (Figure 4(C)). For the study, the above diluted solutions were further adjusted to be 0.5 μg/mL. Immediately after mixing 0.5 μL of the enzyme solutions with 15 μL of the assay solutions carrying the respective substrates (Promega and Wako), the consequent bioluminescence spectra were estimated with the spectrophotometer in an integration time of 5 s.

RESULTS

Artificial Luciferases Differ in Identities from Any Existing Copepod Luciferases. We searched the maximal identities of ALucs, generated with the above-mentioned strategies of CSMS and SSA.

An identity search of ALuc sequences in two famous public databases (NCBI Blast and SIB Blast) revealed that (i) their maximal identities to any existing luciferases were less than 83% by NCBI Blast and 76% by SIB Blast, and (ii) the first and second closest existing luciferases to ALucs were *Metridia pacifica* luciferase (MpLuc) and *Metridia okhotensis* luciferase (MoLuc), respectively.

Optical Properties of ALucs Were Superior to Any Existing Marine Luciferases. The relative optical properties of ALucs compared to major marine luciferases (GLuc, MpLuc1, and RLuc8.6-535) were examined (Figure 1(B)). In general, ALucs exhibited stronger bioluminescence intensities than any existing luciferases, including GLuc and RLuc8.6-535; for instance, **A15**, **A16**, **A23**, and **A25** exhibited 47, 43, 53, and 45 times stronger optical intensities (Figure 1(B)), respectively, and 11 times prolonged bioluminescence than GLuc with native coelenterazine (Figure S4). Further, we estimated the substrate specificity of the made ALucs according to six different coelenterazine variants and compared with RLuc8.6-535 and GLuc. The comparison revealed that ALucs exert a unique substrate selectivity to coelenterazine *i*, whereas RLuc8.6-535 was selective to coelenterazine *ip* (data not shown).

Interestingly, **A18** and **A24** showed a dramatic contrast in optical stability: **A18** quickly lost its activity after an addition of the substrate (only 6.7 (±1.6 s.d.)% at 6 min after the nCTZ injection), whereas **A24** kept 71.2 (±15.3 s.d.)% of its initial activity at 6 min after the nCTZ injection (numbers on bars, Figure 1(B)).

Although the C-terminal ends of **A16**, **A22**, **A23**, and **A25** were all fused with an ER retention signal (KDEL), a relatively higher portion of **A16** and **A23** was secreted to the extracellular matrix (Figure S3(B)). The secreted ratios over the total expression amounts of **A16** and **A23** were 8.8 (±1.2 s.d.)% and 10.1 (±0.5 s.d.)%, respectively. The result shows that **A16** and **A23** exhibit strong secretory properties, which were not fully repressed even by the ER retention signal KDEL. The optical intensities of the secreted luciferases were 89 (±7 s.d.) and 115 (±27 s.d.)-times greater than those of GLuc.

The maximal optical intensities of the ALucs (λ_{max}) were found in the green region of 505−530 nm (Figure 1(B)). The most blue- and red-shifted bioluminescence was found with **A12** (λ_{max} = 500 nm) and **A25** (λ_{max} = 530 nm), respectively.

A22 showed a characteristic instability to heat, compared with the other ALucs. For comparison, we chose four ALucs, **A16**, **A22**, **A23**, and **A25**, whose optical intensities are almost equivalent. Ten minutes after heating **A16**, **A22**, **A23**, and **A25** at 80 °C in a heating block, the enzymatic activity of **A22** decreased to approximately 56% of those of the other ALucs (Figure S3(A)). Our consensus is that the heat stability reflects the poor structural rigidity. To learn more about (i) the 2D structural variance between heat-unstable **A22** and the others and (ii) their putative localization sites, we conducted bioinformatics searches, which results were summarized in the Supporting Information section and Figure S3(C). The overall search results suggest that the N- and C-terminal regions dominate the secretory property and the structural rigidity of ALucs, respectively.

ALucs Exert an Excellent Optical Readout for Two-Hybrid Assays. The suitability of ALucs as an optical readout

was examined with a mammalian two-hybrid assay (Figure 2(A)).

The assay system was designed to commonly carry pACT-MyoD and pBIND-ID (Promega). The only difference in the systems is the reporter expression vector (pG5) encoding GLuc, MpLuc1, **A16**, or **P5**. The normalized fold intensities from the supernatants of the cells carrying pG5-gluc, pG5-mp1, pG5-a16, and pG5-p5 were found to be 1 (±0.3 s.d.), 2 (±0.2 s.d.), 8 (±6.6 s.d.), and 280 (±67.5 s.d.), respectively (Figure 2(A), upper panel). The drastic optical contrast between **P5** and the other reporter proteins shows that a considerable amount of **P5** is secreted to the extracellular matrix, whereas **A16** was strictly retained in the cellular compartments owing to the ER retention signal, 'KDEL'.

Compared with the supernatants, the lysates did not show such a drastic variance in the relative fold intensities, where the relative intensities of the cell lysates carrying pG5-gluc, pG5-mp1, pG5-a16, and pG5-p5 were 1 (±0.5 s.d.), 3 (±2.5 s.d.), 30 (±9.1 s.d.), and 31 (±8.2 s.d.), respectively (Figure 2(A), lower panel). This may be partly caused by an intrinsic false-positive expression of the reporter luciferases from the pG5 vector, which drifts the background intensity, resulting in the relatively smaller signal-to-background (S/B) ratios. The relative fold intensity variances can be partly influenced by the secretion loss of **P5**.

Determination of Cortisol with Single-Chain Probes. The optical properties and ligand sensitivity of single-chain probes carrying split-**A16** were examined (Figure 2(B)).

cSimgr8 and cSimgr9 exhibited relatively higher S/B ratios than the others did in the presence or absence of 10^{-6} M of cortisol, i.e., 15 (±1 s.d.) and 14 (±3 s.d.), respectively (Figure 2(B)). On the other hand, cSimgr13 and cSimgr14 emitted approximately 2 times stronger bioluminescence than the others did, although the S/B ratios were less than those of cSimgr8 and cSimgr9: e.g., the intensities of cSimgr8 and cSimgr13 were 39.5 (±2.8 s.d.) × 10^4 RLU/s and 63.8 (±14.2 s.d.) × 10^4 RLU/s, respectively.

The overall results suggest that (i) any fragment of split-**A16** does not cause a spontaneous complementation in the single chain, and was robust enough to survive in mammalian cells without degradation, and (ii) the optimal dissection sites for **A16** are recommended to make at 125/126 AAs (the split site for cSimgr8) for a better S/B ratio and 146/147 AAs (the split site for cSimgr14) for a better optical intensity.

Live Cell Imaging with Bioluminescence Capsules. The merits of ALucs as an optical readout were further examined with a "bioluminescent capsule", whose basic concept we had previously demonstrated[16] (Figure 3). Figure 3(A) illustrates the molecular structures of new bioluminescent capsules.

The capsule was designed to anchor in the PM with the help of MLS, awaiting apoptosis signals. The fluorescence images of Figure 3(B) show that **P6** is dominantly located in the PM and the ER. The fluorescence image after STS stimulation shows that **P6** is fragmented by capase-3 and diffused into the entire cytosol as intended. The 3D movies are also available on the webpage (Supporting Information), where the locations of **P6** with and without STS were imaged in green (ER tracker) and red (mPlum) fluorescence.

A short-term time course of the bioluminescence of the capsules carrying **A16** was examined with a luminometer (GloMax 20/20n) (Figure 3(C)). After an automatic injection of the substrate nCTZ, **P2** exhibited a relatively weak but growing optical intensity profile, whereas the other capsules exhibited a relatively strong and stable bioluminescence after a characteristic optical spark at around 0.1 s. All the capsules, **P2**, **P4**, **P5**, and **P6**, commonly carry **A16**, but differ in the localization sites: **P2** is sequestered in the ER, unlike **P4**, **P5**, and **P6**. Considering the localization variance between **P2** and the others, the interpretation of the result is that the accessibility of nCTZ differs according to the localization site, which was the determining factor of the time course.

Another short-term kinetics of the bioluminescence for a few seconds according to the capsule localization was further examined with a microplate reader (Corona) after a programmed, automatic injection of the substrate (Figure 3(D)). **P1**, **P2**, and **P6** are designed to locate in the cytosol, the ER, and the PM, respectively. **P1** carrying RLuc8.6-535 exhibited the poorest optical intensities, compared with **P2** and **P6**. Although both **P2** and **P6** commonly carry **A16**, the optical intensities of **P6** were approximately 2 times stronger than those of **P2**. The response time of **P6** (4.4×10^5 RLU/s) was also ca. 6.8 times faster than that of **P2** (6.5×10^4 RLU/s).

A live cell imaging of **P1**, **P3**, and **P4** was carried out with a microslide growing COS-7 cells (Figure 3(E)). The relative optical intensities per area by **P3** and **P4** were ca. 21 times stronger than those by **P1**: the absolute intensities were 375 (±58) RLU/mm^2/s for **P1**, 7951 (±259) RLU/mm^2/s for **P3**, and 8087 (±51) RLU/mm^2/s for **P4**. The magnified optical image suggests that even a living single-cell imaging may be feasible with **P3** or **P4**.

The above results are interpreted as follows: (i) ALucs are an excellent optical ingredient for bioluminescent capsules, whose kinetic study reflects the localization and the substrate accessibility, considering the dramatic variance between **P2** and **P6**; and (ii) conversance of the scheme of bioluminescence capsules with ALucs provides great merits with respect to optical stability, intensity, and the stable supply of the substrate and molecular oxygen (O_2).

ALucs as an Optical Marker for Antibodies. We created a series of **A16**-linked scFv antibodies and compared their optical properties according to the molecular design, including the tags for purification convenience and host organism (Figure 4).

The relative optical intensities of the made antibodies (**A16-v1**, **A16-v2**, and **A16-v3**) and a commercial HRP-linked antibody, **HRP-ab** (GE Healthcare), were compared. HRP-ab was chosen because HRP is the most popular optical readout for antibodies. The comparison reveals that the *E. coli*-expressed **A16-v1** shows the poorest optical intensity among them, implicating the poor folding efficiency. This comparison suggests that an excellent folding environment for **A16** is achieved in mammalian cells, not in *E. coli*. This result is consistent with a previous view that copepod luciferases are rich in the cysteine ratio, and thus the proper folding is hampered in *E. coli*.[10] The optimal folding site is considered at the ER, like other secretion proteins.

The comparison of the relative optical intensities in Figure 4(B) reveals that **A16-v3** exhibits approximately 2 times stronger optical intensities than **HRP-ab**.

The bioluminescence spectra of **A16-v3** and **HRP-ab** were also compared (Figure 4(C)). The λ_{max} of **A16-v3** was 528 nm, where the red light longer than 600 nm to the total (R_{600}) was approximately 15%, whereas the λ_{max} of **HRP-ab** was found to be 492 nm (R_{600} = 6%).

The above results may be summarized as follows: (i) **A16**-linked antibodies are optimally folded in the ER of mammalian cells and secreted to the extracellular matrix, and (ii) the optical properties of **A16** are robust enough not to be significantly hampered by the antibody linkage.

DISCUSSION

The alignments of many relative protein sequences in a database facilitate new insights into their phylogenetic history, common functional motifs, preserved consensus amino acids, and many other features. The CSMS is an excellent example that reveals the merits of sequence alignment. It was designed previously to reveal thermodynamically favored amino acids.[7,17] A more precise bioinformatics analysis of multiple sequence alignments, the SCA, was also conducted to explain the evolutionary constraints and consensus amino acids in the alignments.[9] Further, we had previously suggested an empirical strategy to identify putative active sites of luciferases via a hydrophilicity search and SSA.[5]

The recently advanced approaches guided us in creating a series of ALucs mimicking a consensus sequence of copepod luciferases. Very diverse luciferases in the identities from any existing marine luciferase in the database were practically made.

The present study demonstrates how to create whole sequences of ALucs, instead of identifying several mutation sites in existing luciferases. Fortunately, some of the presently synthesized ALucs exhibited excellent optical properties in intensity and stability. The following are considered success factors: (i) as the sequences of many copepod luciferases have been recently accumulated in the public database,[10] common features on their two-dimensional structures have become more elucidative; (ii) the sequences of copepod luciferases are highly conserved and their nature makes it easy to identify consensus amino acids; and (iii) copepod luciferases have two repeated catalytic domains,[11] whose N- and C-terminal domains are highly conserved and thus alignable to easily identify the variable and consensus amino acids, where we actually tried to increase cases of the consensus amino acids between the N- and C-terminal domains.

We had previously speculated that a hydrophilicity search provides an initial clue for the core region of luciferases.[5] In the present study, our hydrophilicity search on the sequences of ALucs showed a characteristic hydrophilic region between R120 and Q132 of **A16**. A consecutive dissection study also revealed that the fragments of **A16** dissected at E125/G126 exert the highest S/B ratios among those tested. This result is consistent with the above-mentioned hypothesis that we raised on the putative core region.

The poorest optical stability after the substrate addition was found with **A18**. As the optical intensity of **A18** decreased dramatically to 7% of the initial intensity within 6 min (Figure 1), this optical property may be useful as a molecular timer within several minutes or a kinetic reporter. For instance, a new reporter−gene system expressing multiple reporters may be constructed, where each reporter represents different molecular events. In the system, because the prior luminescence quickly disappears, a consecutive bioluminescence assay is possible under a minimal threshold effect by a prior bioluminescence signal.

A22 also exhibited the poorest heat stability among the luciferases made. Although currently insufficient, this heat instability may be utilized as a heat indicator in a future assay system by further modification. This heat instability may be useful for constructing a unique dual reporter−gene assay, where bioluminescence of **A22** may be partly suppressed by heat and a cutoff optical filter, considering that the λ_{max} of **A22** (504 nm) is far from that of **A25** (530 nm). The hydrophilicity variation between the C-terminal regions of **A22** and the others suggests that the heat instability of **A22** may be caused by the hydrophilic amino acids in the C-terminal regions (Figure S3(C)). Further experiments are needed to confirm this speculation.

It is interesting to discuss the peak emission wavelengths (λ_{max}) of ALucs with respect to the light-emitting mechanism of nCTZ. Because nCTZ acts as "chromophore" being oxidized for bioluminescence, the intrinsic optical property of nCTZ should dominate the λ_{max} of bioluminescence. Consensus λ_{max} values with nCTZ among researchers range from 470 to 480 nm. The outstanding red-shifts of λ_{max} were reported with RLuc variants by Loening et al., whose λ_{max} ranged from 486 to 547 nm.[14,18]

In the case of ALucs, the λ_{max} with nCTZ was found to be in the range of 500 to 530 nm, and the photon ratio greater than 600 nm ($9I_{600}$) was ca. 13−15%. These optical properties look reasonable in light of a consensus view of researchers on nCTZ-consuming reactions. The λ_{max} values have been frequently discussed with respect to the hydrophilicity at the binding site of luciferases[19] and the protonation environment of the light emitters during the bioluminescence reaction (i.e., pH).[4] The higher λ_{max} values (i.e., red-shifts) of ALucs than those of other existing marine luciferases suggest that the active site of ALucs provides a relatively hydrophilic environment in the nCTZ-consuming reactions.

The greatest mismatch between the optical properties of ALucs and those of other existing luciferases consuming nCTZ is found in the full width at half maxima (FWHM). FWHMs of ALucs are extraordinarily greater than the conventional consensus on nCTZ-consuming luciferase reactions, e.g., 159 nm for **A16**, 155 nm for **A23**, and 174 nm for **A25**. These FWHMs are approximately 2.5 times greater than those of GLuc and its variants,[15] 2 times higher than Nanoluc and its variants,[20] and 1.5 times broader than those of RLuc and its variants.[14] The broad FWHM of ALucs is considered that plural light emitters are created in the nCTZ-consuming reactions. It is generally accepted that nCTZ can form two possible light emitters, i.e., amide anion and dianion (phenolate anion plus amide anion) of coelenteramide, in the transition state.[21,22] The precedent studies suggest that the present FWHM-broadening feature may be explained by the existence of two (higher and lower) or more stable light emitters in the transition state during the nCTZ-consuming reaction of ALucs. We speculate that at least the two bands by higher and lower light emitters closely overlap in the spectra, and thus the FWHMs are observed to be broadened. A corresponding discussion on the band broadening property of nCTZ-consuming reactions was also discussed in the view of light emitters in a previous paper.[22]

All these considered, we have shown a whole sequence creation of ALucs exerting excellent optical intensity and stability. The sequential identities were clearly different from any existing luciferases. We examined whether ALucs are favorably applicable for existing major bioassays, i.e., reporter-gene assays, single-chain probes, bioluminescent capsules, and bioluminescent antibodies. We can expect a greater and stable bioluminescence in the bioassays, with the conventional reporters being simply replaced with ALucs. The bio-

luminescent capsules are an excellent example of an artificially designed optical reporter to visualize molecular events in the plasma membrane of living mammalian cells under the circumstance of stable supply of the substrate and molecular oxygen (O_2).[16] The capsules show the model structure of future reporter enzymes. The present study provides an approach to create artificial enzymes with designed optical properties for bioassays and encourages researchers to fabricate their own artificial enzymes of interest with designed properties and functionalities.

■ ASSOCIATED CONTENT

Supporting Information

The prototypical sequence of ALuc; Figure S1. Alignments of the N- and C-terminal regions of ALucs and existing copepod luciferases; Figure S2(A) and (B). Heat sensitivity, optical intensities of secreted luciferases, and typical hydrophobicity profiles of the present artificial luciferases, **A22**, **A23**, **A25**; Figure S3. The optical stabilities of ALucs, compared to GLuc; Figure S4. Further, supplementary experimental data is provided: (i) Experimental Procedure for Figure 2(B) (Construction of Single-Chain Probes), (ii) Experimental Procedure for Figure 3(A) (Construction of Bioluminescent Capsules), (iii) Design and Working Mechanism of Bioluminescent Capsules, and (**iv**) Bioinformatics Searches for Figure S3(C) (Construction of Bioluminescent Capsules). Video 1: **P6** without STS: The locations of **P6** without STS were imaged in green (ER tracker) and red (mPlum) fluorescence. The capsule (**P6**) was designed to anchor in the PM with the help of MLS, awaiting apoptosis signals. The fluorescence images in red before STS stimulation show the dominant localization of **P6** in the PM and the ER. Video 2: **P6** with STS: The locations of **P6** with STS were imaged in green (ER tracker) and red (mPlum) fluorescence. The fluorescence image in red after STS stimulation shows that **P6** is fragmented by capase-3 and diffused into the entire cytosol as intended. This material is available free of charge via the Internet at http://pubs.acs.org.

■ AUTHOR INFORMATION

Corresponding Author

*E-mail: kimu-sb@aist.go.jp.

Notes

The authors declare no competing financial interest.

■ REFERENCES

(1) Hastings, J. W. (1996) Chemistries and colors of bioluminescent reactions: a review. *Gene 173*, 5−11.

(2) Viviani, V. R., Uchida, A., Viviani, W., and Ohmiya, Y. (2002) The influence of Ala243 (Gly247), Arg215 and Thr226 (Asn230) on the bioluminescence spectra and pH-sensitivity of railroad worm, click beetle and firefly luciferases. *Photochem. Photobiol. 76*, 538−544.

(3) Nakatsu, T., Ichiyama, S., Hiratake, J., Saldanha, A., Kobashi, N., Sakata, K., and Kato, H. (2006) Structural basis for the spectral difference in luciferase bioluminescence. *Nature 440*, 372−376.

(4) Shimomura, O. (2006) *Bioluminescence*, World Scientific Publishing Co. Pte. Ltd, Singapore.

(5) Kim, S. B. (2012) Labor-effective manipulation of marine and beetle luciferases for bioassays. *Protein Eng. Des. Sel. 25*, 261−269.

(6) Ke, D. C., and Tu, S. C. (2011) Activities, kinetics and emission spectra of bacterial luciferase-fluorescent protein fusion enzymes. *Photochem. Photobiol. 87*, 1346−1353.

(7) Lehmann, M., Loch, C., Middendorf, A., Studer, D., Lassen, S. F., Pasamontes, L., van Loon, A. P. G. M., and Wyss, M. (2002) The consensus concept for thermostability engineering of proteins: further proof of concept. *Protein Eng. 15*, 403−411.

(8) Loening, A. M., Fenn, T. D., Wu, A. M., and Gambhir, S. S. (2006) Consensus guided mutagenesis of *Renilla* luciferase yields enhanced stability and light output. *Protein Eng. Des. Sel. 19*, 391−400.

(9) Russ, W. P., Lowery, D. M., Mishra, P., Yaffe, M. B., and Ranganathan, R. (2005) Natural-like function in artificial WW domains. *Nature 437*, 579−583.

(10) Takenaka, Y., Yamaguchi, A., Tsuruoka, N., Torimura, M., Gojobori, T., and Shigeri, Y. (2012) Evolution of bioluminescence in marine planktonic copepods. *Mol. Biol. Evol. 29*, 1669−1681.

(11) Inouye, S., and Sahara, Y. (2008) Identification of two catalytic domains in a luciferase secreted by the copepod *Gaussia princeps*. *Biochem. Biophys. Res. Commun. 365*, 96−101.

(12) Tannous, B. A., Kim, D. E., Fernandez, J. L., Weissleder, R., and Breakefield, X. O. (2005) Codon-optimized *Gaussia* luciferase cDNA for mammalian gene expression in culture and in vivo. *Mol. Ther. 11*, 435−443.

(13) Takenaka, Y., Masuda, H., Yamaguchi, A., Nishikawa, S., Shigeri, Y., Yoshida, Y., and Mizuno, H. (2008) Two forms of secreted and thermostable luciferases from the marine copepod crustacean, Metridia pacifica. *Gene 425*, 28−35.

(14) Loening, A. M., Wu, A. M., and Gambhir, S. S. (2007) Red-shifted *Renilla reniformis* luciferase variants for imaging in living subjects. *Nat. Methods 4*, 641−643.

(15) Kim, S. B. (2011) Superluminescent variants of marine luciferases. *Anal. Chem. 83*, 8732−8740.

(16) Kim, S. B., Ito, Y., and Torimura, M. (2012) Bioluminescent capsules for live-cell imaging. *Bioconjugate Chem. 23*, 2221−2228.

(17) Steipe, B., Schiller, B., Pluckthun, A., and Steinbacher, S. (1994) Sequence statistics reliably predict stabilizing mutations in a protein domain. *J. Mol. Biol. 240*, 188−192.

(18) Loening, A. M., Dragulescu-Andrasi, A., and Gambhir, S. S. (2010) A red-shifted *Renilla* luciferase for transient reporter-gene expression. *Nat. Methods 7*, 5−6.

(19) Shimomura, O., and Teranishi, K. (2000) Light-emitters involved in the luminescence of coelenterazine. *Luminescence 15*, 51−58.

(20) Hall, M. P., Unch, J., Binkowski, B. F., Valley, M. P., Butler, B. L., Wood, M. G., Otto, P., Zimmerman, K., Vidugiris, G., Machleidt, T., Robers, M. B., Benink, H. A., Eggers, C. T., Slater, M. R., Meisenheimer, P. L., Klaubert, D. H., Fan, F., Encell, L. P., and Wood, K. V. (2012) Engineered luciferase reporter from a deep sea shrimp utilizing a novel imidazopyrazinone substrate. *ACS Chem. Biol. 7*, 1848−1857.

(21) Hori, K., Wampler, J. E., and Cormier, M. J. (1973) Chemiluminescence of *Renilla* (sea pansy) luciferin and its analogs. *J. Chem. Soc., Chem. Commun.*, 492−493.

(22) Giuliani, G., Molinari, P., Ferretti, G., Cappelli, A., Anzini, M., Vomero, S., and Costa, T. (2012) New red-shifted coelenterazine analogues with an extended electronic conjugation. *Tetrahedron Lett. 53*, 5114−5118.